mathematics

MDPI

Article

Approximation-Based Quantized State Feedback Tracking of Uncertain Input-Saturated MIMO Nonlinear Systems with Application to 2-DOF Helicopter

Byung Mo Kim and Sung Jin Yoo *

School of Electrical and Electronics Engineering, Chung-Ang University, 84 Heukseok-Ro, Dongjak-Gu, Seoul 06974, Korea; kimmo1028@cau.ac.kr

* Correspondence: sjyoo@cau.ac.kr

Abstract: This paper addresses an approximation-based quantized state feedback tracking problem of multiple-input multiple-output (MIMO) nonlinear systems with quantized input saturation. A uniform quantizer is adopted to quantize state variables and control inputs of MIMO nonlinear systems. The primary features in the current development are that (i) an adaptive neural network tracker using quantized states is developed for MIMO nonlinear systems and (ii) a compensation mechanism of quantized input saturation is designed by constructing an auxiliary system. An adaptive neural tracker design with the compensation of quantized input saturation is developed by deriving an augmented error surface using quantized states. It is shown that closed-loop stability analysis and tracking error convergence are conducted based on Lyapunov theory. Finally, we give simulation and experimental results of the 2-degrees-of-freedom (2-DOF) helicopter system for verifying to the validity of the proposed methodology where the tracking performance of pitch and yaw angles is measured with the mean squared errors of 0.1044 and 0.0435 for simulation results, and those of 0.0656 and 0.0523 for experimental results.

Keywords: quantized feedback control; state and input quantization; input saturation; MIMO nonlinear systems; 2-DOF helicopter

Citation: Kim, B.M.; Yoo, S.J. Approximation-Based Quantized State Feedback Tracking of Uncertain Input-Saturated MIMO Nonlinear Systems with Application to 2-DOF Helicopter. *Mathematics* **2021**, *9*, 1062. https://doi.org/10.3390/math9091062

Academic Editor: Rami Ahmad El-Nabulsi

Received: 24 March 2021
Accepted: 6 May 2021
Published: 9 May 2021

1. Introduction

In industrial systems, the operating ranges of actuators are restricted because of the physical limitation and specification [1]. The control input saturation closely influences the performance of the control system and the stability of closed-loop systems [2]. Therefore, considerable attention has been devoted to control uncertain nonlinear system in the presence of input saturation. In [3], an adaptive control design approach using the hyperbolic tangent function and the Nussbaum function was presented to compensate for saturation nonlinearities of uncertain nonlinear systems. First-order-filter-based auxiliary systems were introduced to analyze the effect of input saturation in uncertain nonlinear systems such as nonlinear strict-feedback systems [4] and nonlinear stochastic systems [5]. Auxiliary systems using high-order filters were constructed to design adaptive controllers for input-saturated nonlinear systems with model uncertainties such as nonlinear stochastic systems [6] and nonlinear strict-feedback systems [7]. By combining these approaches using auxiliary systems with the function approximation technique, some study results were recently developed for various uncertain nonlinear systems in strict-feedback and pure-feedback forms. In [8], an observer-based adaptive fuzzy tracking controller was designed for nonlinear systems with time delay and input saturation. In [9], a disturbance-observer-based adaptive fuzzy control problem was investigated for nonlinear state constrained systems with input saturation. A robust adaptive control approach was proposed for state-constrained nonlinear systems with input saturation and unknown control direction [10]. Neural-network-based adaptive control problems of pure-feedback nonlinear systems

were addressed using a prescribed performance control technique [11] and a function transformation technique [12]. Furthermore, these adaptive control results were applied to multiple-input multiple-output (MIMO) nonlinear systems with various applications to deal with more practical systems. In [13], an adaptive tracking control was proposed for a class of uncertain MIMO nonlinear systems with non-symmetric input constraints. In [14], the problem of finite-time adaptive fuzzy tracking control was investigated for MIMO nonlinear systems with input saturation. An adaptive neural tracking control problem was studied for MIMO stochastic nonlinear systems with input saturation [15]. In [16], an adaptive backstepping output feedback tracking problem was considered for MIMO stochastic pure-feedback nonlinear systems with input saturation. An adaptive neural tracking control approach was proposed for MIMO pure-feedback time-delay nonlinear systems with input saturation [17]. In [18], an upper limb robotic exoskeleton with input saturation was considered for an adaptive control design. However, the aforementioned study efforts cannot be applied to an adaptive control problem of MIMO nonlinear systems under capacity-limited network environment with state quantization. The primary challenge of this problem is how to deal with the multi-input saturation problem using quantized states in the adaptive control structure and the effects of quantization errors on the system performance.

Network-based control allows reducing reconfiguration and maintenance cost of the controller and improving the control efficiency [19]. Since the digital network resources are limited in the practical communication environment, signal quantization that aims to map a continuous signal into a discrete set has been widely studied for the control problems of nonlinear systems. For a variety of nonlinear systems with input quantization, many interesting study results have been presented. In [20], an adaptive backstepping stabilization problem was considered for nonlinear uncertain systems with input quantization. Adaptive asymptotic tracking control problems were studied for nonlinear uncertain systems with input quantization [21] and actuator faults [22]. In [23], an output feedback control approach was presented for uncertain nonlinear systems with input quantization. In [24], an adaptive backstepping quantized control problem was addressed for a class of nonlinear systems. Furthermore, the input quantization problem has been studied with the input saturation problem to consider both the physical limitation of actuators and lower communication rates. In [25], the problem of adaptive output feedback quantised tracking control was considered for stochastic nonstrict-feedback nonlinear systems with asymmetric input saturation. An adaptive tracking method was presented for a class of uncertain nonlinear systems with input quantization and unknown parameters [26]. However, all the developed control schemes [20–26] only focused on the input quantization problem, namely the state feedback information should be continuously measured for the controller design. To consider state quantization, quantized-states-based adaptive control methods have been recently studied for uncertain nonlinear systems. In [27], an adaptive control problem of matched nonlinear systems was addressed via the backstepping technique. In [28], a command-filtered-based recursive design was introduced for uncertain unmatched nonlinear systems to overcome the discontinuity problem of the derivatives of virtual control laws using quantized states. However, nonlinear functions of systems concerned in [27,28] were assumed to be known and linearly parameterized, i.e., adaptive techniques were only used to deal with parametric uncertainties. To relax this restriction on uncertainties, an approximation-based adaptive tracker in the presence of state quantization and time delays was designed in [29]. In [30], an event-triggered adaptive neural network control approach was studied for nonlinear systems with unknown nonlinearities. However, the resultant nonlinear adaptive control approaches [25–30] involve the following restrictions for more improvement.

(I) The quantized-states-based adaptive control approaches [25–30] focused on the control problems of single-input single-output systems. Since a large number of practical systems possess multivariable characteristics and the stability analysis of MIMO systems is much complicated owing to the interconnected nonlinear dynamics between states and

inputs, the quantized-states-based tracker design methodology for the networked-based control of MIMO nonlinear systems with state quantization needs to be further investigated.

(II) The quantized input saturation problems of uncertain nonlinear systems were considered without state quantization in [25,26] and the input saturation effects were not considered in [27–30]. To the authors' knowledge, there is still no reported work on the input saturation compensation problem in the presence of state quantization. An input saturation compensation strategy using quantized states should be derived for uncertain nonlinear systems with state quantization.

In this work, we propose a quantized-states-based adaptive neural control design for uncertain MIMO nonlinear systems subject to input saturation that overcomes the above restrictions (I) and (II). It is assumed that all system nonlinearities are completely unknown, and the full state variables and control inputs quantized by an uniform quantizer are transmitted to the controller and the MIMO nonlinear systems, respectively. An augmented error surface using auxiliary variables is defined to design a neural-network-based adaptive tracking controller using quantized full state information. The unknown nonlinear functions and quantization errors are compensated by constructing the adaptive tuning laws using quantized states. The compensation signal is introduced with the auxiliary system to attenuate the quantized multi-input saturation influence. Based on the Lyapunov stability theory and some bounding lemmas, the stability of the proposed quantized feedback system is successfully analyzed with the convergence of the tracking error. For a practical application of the proposed theoretical result, we simulate and experiment a 2-degrees-of-freedom (2-DOF) helicopter system.

The rest of the paper is structured as follows. The approximation-based quantized state feedback tracking problem of MIMO nonlinear systems with quantized input saturation is formulated in Section 2. The proposed adaptive quantized control design and its stability analysis are discussed in Section 3. Section 4 introduces a mathematical model of the 2-DOF helicopter system and its simulation and experimental results are presented. Finally, the conclusion is given in Section 5.

2. Problem Statement

Consider a class of uncertain MIMO nonlinear systems with quantized input saturation represented by

$$\begin{aligned} \dot{\boldsymbol{x}}_i &= \boldsymbol{x}_{i+1}, \quad i = 1, \ldots, n-1 \\ \dot{\boldsymbol{x}}_n &= \boldsymbol{f}(\bar{\boldsymbol{x}}_n) + \boldsymbol{g}(\bar{\boldsymbol{x}}_n) u(q(\boldsymbol{v})) \\ \boldsymbol{y} &= \boldsymbol{x}_1 \end{aligned} \tag{1}$$

where $\boldsymbol{x}_i = [x_{i,1}, \ldots, x_{i,m}]^\top \in \mathbb{R}^m$ is the ith state vector, $\bar{\boldsymbol{x}}_n = [x_1^\top, \ldots, x_n^\top]^\top \in \mathbb{R}^{nm}$, $\boldsymbol{y} = [y_1, \ldots, y_m]^\top \in \mathbb{R}^m$ denotes the system output vector, $\boldsymbol{f}(\cdot) \in \mathbb{R}^m$ and $\boldsymbol{g}(\cdot) \in \mathbb{R}^{m \times m}$ are the unknown smooth function vector and matrix, respectively, $\boldsymbol{v} = [v_1, \ldots, v_m]^\top \in \mathbb{R}^m$ is the actual control input vector, $q(\boldsymbol{v}) = [q(v_1), \ldots, q(v_m)]^\top \in \mathbb{R}^m$ is the quantized signal of $\boldsymbol{v}$, and $u(q(\boldsymbol{v})) = [u(q(v_1)), \ldots, u(q(v_m))]^\top \in \mathbb{R}^m$ is the quantized input saturation.

Assumption 1 ([31]). *The matrix $\boldsymbol{g}(\cdot)$ satisfies $0 < \underline{g} \leq |\lambda(\boldsymbol{g}(\cdot))| \leq \bar{g}$, $\forall \bar{\boldsymbol{x}}_n \in \Omega_{\bar{\boldsymbol{x}}_n}$ where $\underline{g} > 0$ and $\bar{g} > 0$ are unknown constants, λ is the eigenvalue operator, and $\Omega_{\bar{\boldsymbol{x}}_n}$ is a compact set.*

The Assumption 1 implies that $\boldsymbol{g}(\cdot)$ is strictly either positive or negative definite. Without losing generality, it is assumed that $\boldsymbol{g}(\cdot) > 0$.

Assumption 2. *The desired signal $\boldsymbol{x_d}(t) = [x_{1,d}, \ldots x_{m,d}] \in \mathbb{R}^m$ is continuously differentiable up to the nth order, bounded, and available for the controller design.*

In this paper, the network-based control environment with state and input quantization is considered for the system (1). As the input and state quantizer, the uniform quantizer is selected by the following function

$$h^q \triangleq q(h) = \begin{cases} L_\iota, & L_\iota - \frac{l}{2} \le h < L_\iota + \frac{l}{2} \\ 0, & -\frac{l}{2} \le h < \frac{l}{2} \\ -L_\iota, & -L_\iota - \frac{l}{2} \le h < -L_\iota + \frac{l}{2} \end{cases} \tag{2}$$

where $h = x_{i,j}, v_j$ with $i = 1, \ldots, n$ and $j = 1, \ldots, m$, $\iota \in \mathbb{Z}^+$, l means the length of the quantization interval, $L_1 = l$, and $L_{\iota+1} = L_\iota + l$. Hence, the state and input quantization errors $\delta_{x_{i,j}} \triangleq x_{i,j} - x^q_{i,j}$ and $\delta_{v_j} \triangleq v_j - v^q_j$ satisfy $|\delta_{x_{i,j}}| \le l$ and $|\delta_{v_j}| \le l$, respectively [32].

Assumption 3 ([27]). *The quantized state vector $\boldsymbol{x}^q_i = [x^q_{i,1}, \ldots, x^q_{i,m}]^\top$, $i = 1, \ldots, n$, is available for feedback instead of the state vector $\boldsymbol{x}_i$.*

Remark 1. *According to quantization levels, there exist various quantizers such as uniform quantizer, hysteresis-uniform quantizer, logarithmic-uniform quantizer, etc. In this paper, we use the uniform quantizer (2) for the simple analysis and implementation, as states and input quantizers. However, the uniform quantizers can be easily replaced with other quantizers in our control design.*

The saturation of the jth quantized input $u(v^q_j)$ is described by

$$u(v^q_j) = \mathrm{sat}(v^q_j) = \begin{cases} \mathrm{sign}(v^q_j) u_{j,M}, & |v^q_j| \ge u_{j,M} \\ v^q_j, & |v^q_j| < u_{j,M} \end{cases} \tag{3}$$

where $j = 1, \ldots, m$, $u_{j,M}$ is the saturation bound of v^q_j, and $\mathrm{sign}(\cdot)$ denotes the sign function.

Lemma 1 ([33]). *For any $\epsilon > 0$ and $s \in \mathbb{R}$, it is ensured that $0 \le |s| - s\tanh(s/\epsilon) \le 0.2785\epsilon$.*

Problem 1. *The aim of this study is to design a quantized-states-based adaptive control vector $\boldsymbol{v}$ for uncertain MIMO nonlinear systems (1) ensuring that the output $\boldsymbol{y}$ follows the desired signal $\boldsymbol{x}_d$ in the presence of quantized input saturation.*

3. Adaptive Neural Tracking Control in the Presence of State Quantization and Quantized Input Saturation

3.1. Quantized-States-Based Adaptive Tracker Design Using Neural Networks

To achieve the presented adaptive tracking control objective, we define an augmented error vector $\boldsymbol{s}$ given by

$$\boldsymbol{s} = \left(\frac{d}{dt} + \boldsymbol{\Lambda}\right)^{n-1} \boldsymbol{z}_1 = \sum_{k=0}^{n-1} \binom{n-1}{k} \boldsymbol{\Lambda}^k \boldsymbol{z}_{n-k} \tag{4}$$

where $\boldsymbol{s} = [s_1, \ldots, s_m]^\top \in \mathbb{R}^m$, $\boldsymbol{z}_i = \boldsymbol{x}_i - \boldsymbol{x}^{(i-1)}_d$, $i = 1, \ldots, n-1$, $\boldsymbol{z}_n = \boldsymbol{x}_n - \boldsymbol{x}^{(n-1)}_d - \boldsymbol{\Psi}\mathrm{Tanh}\boldsymbol{\phi}$, $\boldsymbol{\Lambda} = \mathrm{diag}[\lambda_1, \ldots, \lambda_m]$ with constants $\lambda_j > 0$, $j = 1, \ldots, m$, and $\binom{n-1}{k}$ denote binomial coefficients. Here, $\boldsymbol{\Psi} = \mathrm{diag}[\psi_1, \ldots, \psi_m]$; $\psi_j > 0$, $j = 1, \ldots, m$, are constants, $\mathrm{Tanh}\boldsymbol{\phi} = [\tanh\phi_1, \ldots, \tanh\phi_m]$, and ϕ_j, $j = 1, \ldots, m$, are the compensation variables to deal with the influence of input saturation to be designed later.

Remark 2. *Compared with the existing works related to the input saturation [8–18], the compensation variable vector $\boldsymbol{\phi}$ employed in the error surface $\boldsymbol{z}_n = \boldsymbol{x}_n - \boldsymbol{x}^{(n-1)}_d - \boldsymbol{\Psi}\mathrm{Tanh}\boldsymbol{\phi}$ is provided by an auxiliary system using the quantized state feedback information in order to overcome the quantized input saturation problem. Furthermore, the tanh function form is used to ensure the boundedness of the compensation signal $\boldsymbol{\phi}$.*

From (4), the time derivative of $\boldsymbol{s}$ is

$$\dot{\boldsymbol{s}} = \sum_{k=1}^{n-1} \binom{n-1}{k} \boldsymbol{\Lambda}^k \boldsymbol{z}_{n-k+1} + \boldsymbol{f}(\bar{\boldsymbol{x}}) + \boldsymbol{g}(\bar{\boldsymbol{x}}) u(\boldsymbol{v}^q) - \boldsymbol{\Psi} Cosh_I(\boldsymbol{\phi}) \dot{\boldsymbol{\phi}} - \boldsymbol{x}_d^{(n)} \tag{5}$$

where $Cosh_I(\boldsymbol{\phi}) = \mathrm{diag}[1/cosh^2(\phi_1), \ldots, 1/cosh^2(\phi_m)]$ and $u(\boldsymbol{v}^q) = [u(v_1^q), \ldots, u(v_m^q)]^\top$.

A Lyapunov function is defined as $V = (1/2)\boldsymbol{s}^\top \boldsymbol{s}$. Then, the time derivative of V along (2) and (5) becomes

$$\dot{V} = \boldsymbol{s}^\top \left(\sum_{k=1}^{n-1} \binom{n-1}{k} \boldsymbol{\Lambda}^k \boldsymbol{z}_{n-k+1} + \boldsymbol{f}(\bar{\boldsymbol{x}}) + \boldsymbol{g}(\bar{\boldsymbol{x}}) u(\boldsymbol{v}^q) - \boldsymbol{\Psi} Cosh_I(\boldsymbol{\phi}) \dot{\boldsymbol{\phi}} - \boldsymbol{x}_d^{(n)} \right). \tag{6}$$

Here, unknown nonlinear function vector $\boldsymbol{f}(\bar{\boldsymbol{x}})$ can be approximated via the universal approximation property of radial basis function neural networks (RBFNNs) [34] in the compact set $\mho \subset \mathbb{R}^{nm}$ as follows:

$$\boldsymbol{f}(\bar{\boldsymbol{x}}) = \boldsymbol{W}^\top \boldsymbol{Q}(\bar{\boldsymbol{x}}) + \boldsymbol{\varepsilon}(\bar{\boldsymbol{x}}), \quad \bar{\boldsymbol{x}} \in \mho \tag{7}$$

where $\boldsymbol{W} = \mathrm{diag}[\boldsymbol{W}_1, \ldots, \boldsymbol{W}_m] \in \mathbb{R}^{mM \times m}$ is the ideal bounded weighting matrix, $\boldsymbol{W}_j = [W_{j,1}, \ldots, W_{j,M}]^\top$, $j = 1, \ldots, m$, satisfying $\|\boldsymbol{W}_j\| \leq \bar{W}_j$ with constants $\bar{W}_j > 0$, M is the number of neural nodes, $\boldsymbol{\varepsilon} \in \mathbb{R}^m$ represents an approximation reconstruction error such that $\|\boldsymbol{\varepsilon}\| \leq \bar{\varepsilon}$ with an unknown constant $\bar{\varepsilon} > 0$, $\boldsymbol{Q} = [\boldsymbol{Q}_1^\top, \ldots, \boldsymbol{Q}_m^\top]^\top \in \mathbb{R}^{mM}$ denotes the Gaussian function vector with $\boldsymbol{Q}_j \in \mathbb{R}^M$, $j = 1, \ldots, m$. The vector $\boldsymbol{Q}_j$ is bounded as $\|\boldsymbol{Q}_j\| \leq \bar{Q}_j$ with a constant $\bar{Q}_j > 0$ from the inherent property of Gaussian basis functions [35,36].

By employing (7) to estimate $\boldsymbol{f}(\bar{\boldsymbol{x}})$ and defining an un-quantized signal $\check{\boldsymbol{v}}$, (6) becomes

$$\begin{aligned} \dot{V} = \boldsymbol{s}^\top \Bigg(& \sum_{k=1}^{n-1} \binom{n-1}{k} \boldsymbol{\Lambda}^k \boldsymbol{z}_{n-k+1} + \boldsymbol{W}^\top \boldsymbol{Q}(\bar{\boldsymbol{x}}) + \boldsymbol{\varepsilon}(\bar{\boldsymbol{x}}) + \boldsymbol{g}(\bar{\boldsymbol{x}}) u(\boldsymbol{v}^q) + \check{\boldsymbol{v}} - \boldsymbol{v} \\ & + (\boldsymbol{v} - \check{\boldsymbol{v}}) - \boldsymbol{\Psi} Cosh_I(\boldsymbol{\phi}) \dot{\boldsymbol{\phi}} - \boldsymbol{x}_d^{(n)} \Bigg). \end{aligned} \tag{8}$$

Then, $\check{\boldsymbol{v}}$ is chosen as

$$\check{\boldsymbol{v}} = -\boldsymbol{\zeta} \boldsymbol{s} - \sum_{k=1}^{n-1} \binom{n-1}{k} \boldsymbol{\Lambda}^k \boldsymbol{z}_{n-k+1} + \boldsymbol{x}_d^{(n)} - \hat{\boldsymbol{W}}^\top \boldsymbol{Q}(\bar{\boldsymbol{x}}) - \hat{B} \mathrm{Tanh}(\boldsymbol{s}/\epsilon) \tag{9}$$

where $\mathrm{Tanh}(\boldsymbol{s}/\epsilon) = [\tanh(s_1/\epsilon_1), \ldots, \tanh(s_m/\epsilon_m)]^\top \in \mathbb{R}^m$, $\boldsymbol{\zeta} = \mathrm{diag}[\zeta_1, \ldots, \zeta_m]; \zeta_j > 0$, $\epsilon_j > 0, j = 1, \ldots, m$, are design constants, $\hat{\boldsymbol{W}} = \mathrm{diag}[\hat{\boldsymbol{W}}_1, \ldots, \hat{\boldsymbol{W}}_m]$; $\hat{\boldsymbol{W}}_j = [\hat{W}_{j,1}, \ldots, \hat{W}_{j,M}]^\top$, $j = 1, \ldots, m$, and $\hat{B}$ are estimates of $\boldsymbol{W}_j$ and B, respectively. Here, the positive unknown constant B is derived later.

Applying (9) into (8) gives

$$\begin{aligned} \dot{V} = & -\boldsymbol{s}^\top \boldsymbol{\zeta} \boldsymbol{s} - \boldsymbol{s}^\top \tilde{\boldsymbol{W}}^\top \boldsymbol{Q}(\bar{\boldsymbol{x}}) + \boldsymbol{s}^\top \boldsymbol{\varepsilon}(\bar{\boldsymbol{x}}) + \boldsymbol{s}^\top (\boldsymbol{g}(\bar{\boldsymbol{x}}) u(\boldsymbol{v}^q) - \boldsymbol{v} - \boldsymbol{\Psi} Cosh_I(\boldsymbol{\phi}) \dot{\boldsymbol{\phi}}) \\ & + \boldsymbol{s}^\top (\boldsymbol{v} - \check{\boldsymbol{v}}) - \tilde{B} \boldsymbol{s}^\top \mathrm{Tanh}(\boldsymbol{s}/\epsilon) - B \boldsymbol{s}^\top \mathrm{Tanh}(\boldsymbol{s}/\epsilon) \end{aligned} \tag{10}$$

where $\tilde{\boldsymbol{W}} = \hat{\boldsymbol{W}} - \boldsymbol{W}$ and $\tilde{B} = \hat{B} - B$ are the estimation errors.

To construct a quantized-states-based actual control law $\boldsymbol{v}$, a quantized-states-based augmented error $\boldsymbol{s}^*$ is defined as

$$\boldsymbol{s}^* = \sum_{k=0}^{n-1} \binom{n-1}{k} \boldsymbol{\Lambda}^k \boldsymbol{z}_{n-k}^* \tag{11}$$

where the error surfaces z_i^*, $i = 1, \ldots, n$, with quantized state variables are given by

$$\begin{aligned} z_i^* &= x_i^q - x_d^{(i-1)}, \quad i = 1, \ldots, n-1, \\ z_n^* &= x_n^q - x_d^{(n-1)} - \Psi \mathrm{Tanh}\boldsymbol{\phi} \end{aligned} \tag{12}$$

where $x_j^q = [x_{j,1}^q, \ldots, x_{j,m}^q]^\top$, $j = 1, \ldots, m$, and the saturation compensation vector $\boldsymbol{\phi} = [\phi_1, \ldots, \phi_m]^\top$ is provided by the following auxiliary system using quantized states

$$\dot{\phi}_j = (\cosh^2 \phi_j)(-\kappa_j \tanh \phi_j + u(v_j^q) - v_j^q)/\psi_j, \quad \phi_j(0) = 0, \quad j = 1, \ldots, m, \tag{13}$$

with a design constant $\kappa_j > 0$.

Based on the quantized-states-based augmented error s^*, we propose an actual control law v with adaptation laws for $\hat{W}_j$ and $\hat{B}$ as follows:

$$v = -\zeta s^* - \sum_{k=1}^{n-1} \binom{n-1}{k} \Lambda^k z_{n-k+1}^* + x_d^{(n)} - \hat{W}^\top Q(\bar{x}^q) - \hat{B}\mathrm{Tanh}(s^*/\epsilon) \tag{14}$$

$$\dot{\hat{W}}_j = \Gamma_{W,j}(s_j^* Q_j(\bar{x}^q) - \sigma_W |s_j^*| \hat{W}_j), \quad j = 1, \ldots, m \tag{15}$$

$$\dot{\hat{B}} = \Gamma_B(s^{*\top} \mathrm{Tanh}(s^*/\epsilon) - \sigma_B \|s^*\| \hat{B}) \tag{16}$$

where $\bar{x}^q = [(x_1^q)^\top, \ldots, (x_n^q)^\top]^\top$, $\Gamma_{W,j} = \mathrm{diag}[\gamma_{w,j,1}, \ldots, \gamma_{w,j,M}]$; $\gamma_{w,j,i} > 0$, $i = 1, \ldots, M$, and $\Gamma_B > 0$ are tuning gains, $\sigma_W > 0$ and $\sigma_B > 0$ are small constants for σ-modification, and s_j^* is the jth element of s^*.

Substituting (13) into (10) yields

$$\begin{aligned} \dot{V} = &-s^\top \zeta s - s^\top \tilde{W}^\top Q(\bar{x}) + s^\top \varepsilon(\bar{x}) + s^\top (g(\bar{x})u(v^q) - u(v^q) + \kappa \mathrm{Tanh}\boldsymbol{\phi} - \delta_v) \\ &+ s^\top (v - \check{v}) - \tilde{B} s^\top \mathrm{Tanh}(s/\epsilon) - B s^\top \mathrm{Tanh}(s/\epsilon) \end{aligned} \tag{17}$$

where $\kappa = \mathrm{diag}[\kappa_1, \ldots, \kappa_m]$ and $\delta_v = v - v^q$.

Using Assumption 1, (3), and Young's inequality, we have

$$\begin{aligned} s^\top (g(\bar{x})u(v^q) - u(v^q)) &\le \|s\|(\bar{g} + 1)u_M \\ s^\top \kappa \mathrm{Tanh}\boldsymbol{\phi} &\le \|s\|\bar{\kappa} \\ -s^\top \delta_v &\le \|s\|\sqrt{m}l \end{aligned}$$

where $\bar{\kappa} = \sqrt{\sum_{j=1}^m \kappa_j^2}$ and $u_M = \sqrt{\sum_{j=1}^m u_{j,M}^2}$. Then, (17) becomes

$$\begin{aligned} \dot{V} \le &-s^\top \zeta s - s^\top \tilde{W}^\top Q(\bar{x}) + s^\top \varepsilon(\bar{x}) + \|s\|((\bar{g} + 1)u_M + \bar{\kappa} + \sqrt{m}l) \\ &+ s^\top (v - \check{v}) - \tilde{B} s^\top \mathrm{Tanh}(s/\epsilon) - B s^\top \mathrm{Tanh}(s/\epsilon). \end{aligned} \tag{18}$$

Remark 3. *In the previous adaptive control design to deal with quantized input saturation problem [25,26], the state quantization problem was not considered. Different from [25,26], the quantized state variables $\bar{x}^q$ are used in the proposed control law (14) instead of original states variables $\bar{x}$. Thus, the stability analysis for quantization signal errors between original states and quantized states are necessary. In the proposed quantized-states-based adaptive tracking control structure shown in Figure 1, the compensation term $\Psi \mathrm{Tanh}\boldsymbol{\phi}$ provided by the auxiliary system (13) is adopted in the augmented error (11) and control law (14) to compensate for multi-input saturation effects. To compensate for system uncertainties and unknown parameters, the quantized-states-based neural network $\hat{W}^\top Q(\bar{x}^q)$ and parameter adaptation laws (15) and (16) are derived for uncertain MIMO nonlinear systems. The closed-loop stability is analyzed by establishing the boundedenss of quantization errors in the next subsection.*

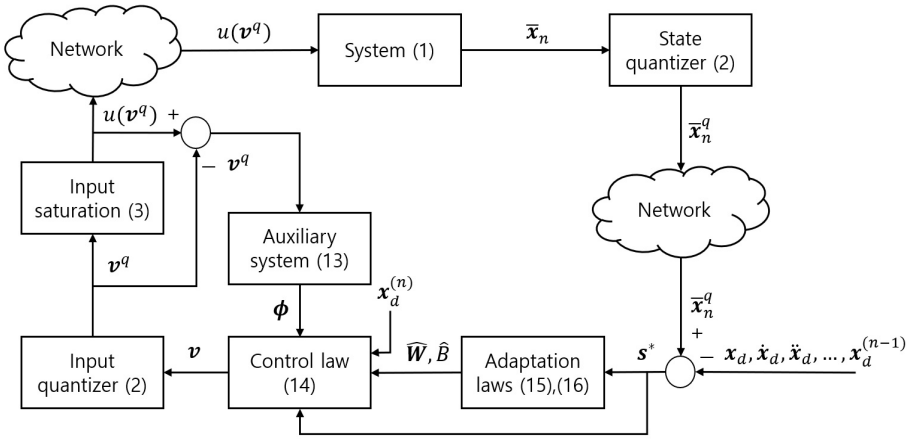

Figure 1. Block diagram of the proposed quantized-states-based adaptive tracking system in the presence of quantized input saturation.

3.2. Quantization Errors and Closed-Loop Stability Analysis

In this section, the stability analysis of the closed-loop system is carried out by Lyapunov theory.

Lemma 2. *For the adaptation law* (15)*, there exists a compact set* $\Omega_{W_j} = \{\tilde{\boldsymbol{W}}_j | \|\tilde{\boldsymbol{W}}_j\| \leq \Xi_{W_j}\}$ *with an unknown constant* Ξ_{W_j} *such that* $\tilde{\boldsymbol{W}}_j(t) \in \Omega_{W_j}$ *for all* $t \geq 0$ *provided that* $\tilde{\boldsymbol{W}}_j(0) \in \Omega_{W_j}$ *where* $j = 1, \ldots, m$*.*

Proof. Consider a Lyapunov function candidate $V_{W_j} = (1/2)\tilde{\boldsymbol{W}}_j^\top \boldsymbol{\Gamma}_{W,j}^{-1} \tilde{\boldsymbol{W}}_j$. Then, differentiating V_{W_j} with respect to time gives

$$\dot{V}_{W_j} = \tilde{\boldsymbol{W}}_j^\top (s_j^* \boldsymbol{Q}_j(\bar{\boldsymbol{x}}^q) - \sigma_W |s_j^*| \hat{\boldsymbol{W}}_j) = \tilde{\boldsymbol{W}}_j{}^\top (s_j^* \boldsymbol{Q}_j(\bar{\boldsymbol{x}}^q) - \sigma_W |s_j^*| (\tilde{\boldsymbol{W}}_j + \boldsymbol{W}_j)). \tag{19}$$

Since there exist constants $\bar{W}_j$ and $\bar{Q}$ such that $\|\boldsymbol{W}_j\| \leq \bar{W}_j$ and $\|\boldsymbol{Q}_j\| \leq \bar{Q}_j$, respectively, $\dot{V}_{W_j}$ becomes

$$\dot{V}_{W_j} \leq \|\tilde{\boldsymbol{W}}_j\| |s_j^*| (\bar{Q}_j + \sigma_W \bar{W}_j - \sigma_W \|\tilde{\boldsymbol{W}}_j\|). \tag{20}$$

From (20), $\dot{V}_{W_j} < 0$ when $\|\tilde{\boldsymbol{W}}_j\| > \Xi_{W_j}$ with $\Xi_{W_j} = (\bar{Q}_j + \sigma_W \bar{W}_j)/\sigma_W$. Thus, $\tilde{\boldsymbol{W}}_j$ are bounded within Ω_{W_j}. Thus, if $\tilde{\boldsymbol{W}}_j(0) \in \Omega_{W_j}$, it holds that $\tilde{\boldsymbol{W}}_j(t) \in \Omega_{W_j}$ for all $t \geq 0$. □

Lemma 3. *For the adaptation law* (16)*. there exists a compact set* $\Omega_B = \{\tilde{B} | |\tilde{B}| \leq \Xi_B\}$ *with an unknown constant* Ξ_B *such that* $\tilde{B}(t) \in \Omega_B$ *for all* $t \geq 0$ *provided that* $\tilde{B}(0) \in \Omega_B$*.*

Proof. Consider $V_B = (1/2)\tilde{B}^2/\Gamma_B$. From $\|\mathrm{Tanh}(\boldsymbol{s}^*/\epsilon)\| \leq \sqrt{m}$ and $\hat{B} = B + \tilde{B}$, $\dot{V}_B$ is represented by

$$\dot{V}_B \leq |\tilde{B}| \|\boldsymbol{s}^*\| (\sqrt{m} + \sigma_B B - \sigma_B |\tilde{B}|). \tag{21}$$

Then, by defining $\Xi_B \triangleq (\sqrt{m} + \sigma_B B)/\sigma_B$ and reasoning the proof of Lemma 2, $\tilde{B}(t) \in \Omega_B$, $\forall t \geq 0$ is ensured if $\tilde{B}(0) \in \Omega_B$. □

Lemma 4. *Define the quantization errors of the augmented error surface and the control input vector as*

$$\boldsymbol{\delta}_s = \boldsymbol{s} - \boldsymbol{s}^*, \quad \boldsymbol{\delta}_{\breve{v}} = \breve{\boldsymbol{v}} - \boldsymbol{v}. \tag{22}$$

Then, there exist positive constants Δ_s and $\Delta_{\breve{\sigma}}$ such that $\|\boldsymbol{\delta}_s\| \leq \Delta_s$ and $\|\boldsymbol{\delta}_{\breve{\sigma}}\| \leq \Delta_{\breve{\sigma}}$, respectively.

Proof. Define $\boldsymbol{\delta}_Q = \boldsymbol{Q}(\bar{\boldsymbol{x}}) - \boldsymbol{Q}(\bar{\boldsymbol{x}}^q)$ and $\boldsymbol{\delta}_t = \mathrm{Tanh}(\boldsymbol{s}/\epsilon) - \mathrm{Tanh}(\boldsymbol{s}^*/\epsilon)$. From $\|\boldsymbol{Q}_j\| \leq \bar{Q}_j$, there exists a constant $\bar{Q}$ such that $\|\boldsymbol{Q}\| \leq \bar{Q}$. Using $\|\mathrm{Tanh}(\cdot)\| \leq \sqrt{m}$, we obtain the inequalities $\|\boldsymbol{\delta}_Q\| \leq 2\bar{Q}$ and $\|\boldsymbol{\delta}_t\| \leq 2\sqrt{m}$. Using the property $|\delta_{x_{i,j}}| \leq l$, $\boldsymbol{\delta}_s$ becomes

$$\begin{aligned}\|\boldsymbol{\delta}_s\| &= \left\| \sum_{k=0}^{n-1} \binom{n-1}{k} \boldsymbol{\Lambda}^k \boldsymbol{z}_{n-k} - \sum_{k=0}^{n-1} \binom{n-1}{k} \boldsymbol{\Lambda}^k \boldsymbol{z}^*_{n-k} \right\| \\ &= \left\| \sum_{k=0}^{n-1} \binom{n-1}{k} \boldsymbol{\Lambda}^k (\boldsymbol{x}_{n-k} - \boldsymbol{x}^q_{n-k}) \right\| \\ &\leq \left\| \sum_{k=0}^{n-1} \binom{n-1}{k} \boldsymbol{\Lambda}^k l\sqrt{m} \right\| \triangleq \Delta_s. \end{aligned} \tag{23}$$

Thus, using (9) and (14), $\boldsymbol{\delta}_{\breve{\sigma}}$ is obtained as

$$\boldsymbol{\delta}_{\breve{\sigma}} = -\boldsymbol{\zeta}\boldsymbol{\delta}_s - \sum_{k=1}^{n-1} \binom{n-1}{k} \boldsymbol{\Lambda}^k (\boldsymbol{z}_{n-k+1} - \boldsymbol{z}^*_{n-k+1}) - \hat{\boldsymbol{W}}^\top \boldsymbol{\delta}_Q - \hat{B}\boldsymbol{\delta}_t. \tag{24}$$

Using Lemmas 2 and 3, $\boldsymbol{\delta}_{\breve{\sigma}}$ is bounded as

$$\|\boldsymbol{\delta}_{\breve{\sigma}}\| \leq \|\boldsymbol{\zeta}\|\Delta_s + \sum_{k=1}^{n-1} \binom{n-1}{k} \|\boldsymbol{\Lambda}\|^k l\sqrt{m} + 2\bar{Q} \sum_{j=1}^{m} (\Xi_{W_j} + \bar{W}_j) + 2\sqrt{m}(\Xi_B + B) \triangleq \Delta_{\breve{\sigma}}. \tag{25}$$

Thus, it is ensured that $\|\boldsymbol{\delta}_s\| \leq \Delta_s$ and $\|\boldsymbol{\delta}_{\breve{\sigma}}\| \leq \Delta_{\breve{\sigma}}$. □

Based on Lemmas 2–4, the main result of our study is presented as follows.

Theorem 1. *Consider the uncertain MIMO nonlinear system (1) with state quantization and quantized input saturation controlled by the proposed adaptive quantized state feedback tracker consisting of (13)–(16). Then, all closed-loop signals are uniformly ultimately bounded and the tracking error z_1 converges to an adjustable neighborhood of the origin.*

Proof. From (18) and $\|\boldsymbol{\delta}_{\breve{\sigma}}\| \leq \Delta_{\breve{\sigma}}$, the time derivative of V is

$$\begin{aligned}\dot{V} \leq &-\boldsymbol{s}^\top \boldsymbol{\zeta}\boldsymbol{s} - \boldsymbol{s}^\top \tilde{\boldsymbol{W}}^\top \boldsymbol{Q}(\bar{\boldsymbol{x}}) + \boldsymbol{s}^\top \boldsymbol{\varepsilon}(\bar{\boldsymbol{x}}) + \|\boldsymbol{s}\|((\bar{g}+1)u_M + \bar{\kappa} + \sqrt{m}l + \Delta_{\breve{\sigma}}) \\ &- \tilde{B}\boldsymbol{s}^\top \mathrm{Tanh}(\boldsymbol{s}/\epsilon) - B\boldsymbol{s}^\top \mathrm{Tanh}(\boldsymbol{s}/\epsilon). \end{aligned} \tag{26}$$

Owing to $\|\boldsymbol{\varepsilon}\| < \bar{\varepsilon}$ with a constant $\bar{\varepsilon}$ and the boundedness of $\tilde{\boldsymbol{W}}$ from Lemma 2, (26) becomes

$$\begin{aligned}\dot{V} \leq &-\boldsymbol{s}^\top \boldsymbol{\zeta}\boldsymbol{s} + \|\boldsymbol{s}\| \left((\bar{g}+1)u_M + \bar{\kappa} + \sqrt{m}l + \Delta_{\breve{\sigma}} + \bar{Q} \sum_{j=1}^{m} \Xi_{W_j} + \bar{\varepsilon} \right) \\ &- \tilde{B}\boldsymbol{s}^\top \mathrm{Tanh}(\boldsymbol{s}/\epsilon) - B\boldsymbol{s}^\top \mathrm{Tanh}(\boldsymbol{s}/\epsilon). \end{aligned} \tag{27}$$

By defining $B = (\bar{g}+1)u_M + \bar{\kappa} + \sqrt{m}l + \Delta_{\breve{\sigma}} + \bar{Q}\sum_{j=1}^{m} \Xi_{W_j} + \bar{\varepsilon}$ and using Lemma 1, we obtain the following inequality

$$-B\boldsymbol{s}^\top \mathrm{Tanh}(\boldsymbol{s}/\epsilon) + B\|\boldsymbol{s}\| \leq \sum_{j=1}^{m} B(|s_j| - s_j \tanh(s_j/\epsilon_j)) \leq \sum_{j=1}^{m} 0.2785 B\epsilon_j. \tag{28}$$

Additionally, using the inequality $|\tilde{B}\boldsymbol{s}^\top \mathrm{Tanh}(\boldsymbol{s}/\epsilon)| \leq \|\boldsymbol{s}\|^2/2 + (\Xi_B)^2/2$ and selecting the design parameter as $\boldsymbol{\zeta} = (1/2)\boldsymbol{I} + \bar{\zeta}\boldsymbol{I}$ with an identity matrix $\boldsymbol{I} \in \mathbb{R}^{m\times m}$ and a positive constant $\bar{\zeta}$, (27) can be represented by

$$\dot{V} \leq -\bar{\zeta}V + C \tag{29}$$

where $C = (\Xi_B)^2/2 + \sum_{j=1}^{m} 0.2785B\epsilon_j$. Integrating both sides of (29), the following inequality holds

$$V(t) \leq V(0)e^{-\bar{\zeta}t} + \frac{C}{\bar{\zeta}}(1 - e^{-\bar{\zeta}t}), \quad \forall t \geq 0. \tag{30}$$

This inequality demonstrates that $V(t)$ is eventually bounded within the value $C/\bar{\zeta}$ which can be reduced arbitrarily small. Thus, all the closed-loop signals are uniformly ultimately bounded. Since $\boldsymbol{s}$ is bounded, the tracking error vector $\boldsymbol{z}_1$ is also bounded. Furthermore, the control law $\boldsymbol{v}$ is bounded and thus $\|u(\boldsymbol{v}^q) - \boldsymbol{v}^q\| \leq \varsigma$ is ensured with a constant ς. From this fact, we can check the boundedness of the auxiliary system variable $\boldsymbol{\phi}$ by defining the Lyapunov function candidate $V_\phi = (1/2)\boldsymbol{\phi}^\top \boldsymbol{\Psi}\boldsymbol{\phi}$. Then, the time derivative of V_ϕ along (13) is represented by

$$\begin{aligned} \dot{V}_\phi &= \cosh^\top \boldsymbol{\phi} \cosh \boldsymbol{\phi}(-\boldsymbol{\phi}^\top \boldsymbol{\kappa}\mathrm{Tanh}\boldsymbol{\phi} + \boldsymbol{\phi}^\top (u(\boldsymbol{v}^q) - \boldsymbol{v}^q)) \\ &\leq \cosh^\top \boldsymbol{\phi} \cosh \boldsymbol{\phi}[\underline{\kappa}(\|\boldsymbol{\phi}\| - \boldsymbol{\phi}^\top \tanh \boldsymbol{\phi}) - \underline{\kappa}\|\boldsymbol{\phi}\| + \varsigma\|\boldsymbol{\phi}\|] \end{aligned} \tag{31}$$

where $\cosh \boldsymbol{\phi} = [\cosh \phi_1, \ldots, \cosh \phi_m]^\top$ and $\underline{\kappa} = \min\{\kappa_1, \ldots, \kappa_m\}$.

By choosing $\underline{\kappa} = \varsigma + \underline{\kappa}^*$ with a constant $\underline{\kappa}^* > 0$, (31) becomes

$$\dot{V}_\phi \leq \cosh^\top \boldsymbol{\phi} \cosh \boldsymbol{\phi}(0.2785m\underline{\kappa} - \underline{\kappa}^*\|\boldsymbol{\phi}\|) \tag{32}$$

From (32), $\dot{V}_\phi < 0$ when $\|\boldsymbol{\phi}\| > 0.2785m\underline{\kappa}/\underline{\kappa}^*$. Thus, owing to $\boldsymbol{\phi}(0) = 0$, $\boldsymbol{\phi}$ is bounded in a compact set $\Xi_\phi = \{\boldsymbol{\phi}(t) | \|\boldsymbol{\phi}(t)\| \leq 0.2785m\underline{\kappa}/\underline{\kappa}^*\}, \forall t \geq 0$. □

4. Application to 2-DOF Helicopter

A 2-DOF helicopter system shown in Figure 2 is a twin rotor experiment equipment for advanced aerospace applications. The helicopter system driven by two DC motor consists of a main rotor that controls the pitch and a tail rotor that controls the yaw where each angle is measured by its encoder. The 2-DOF helicopter system is simulated and experimented to illustrate the effectiveness of the proposed control approach.

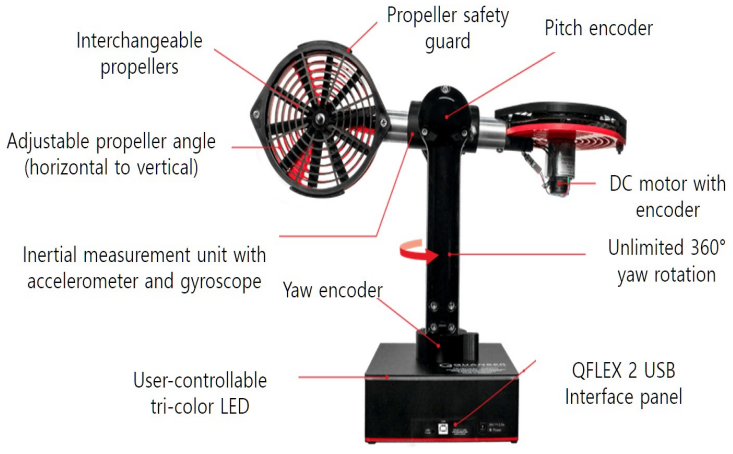

Figure 2. Quanser Aero 2-DOF Helicopter [37].

4.1. Mathematical Model

The dynamics of the 2-DOF helicopter system is represented by the following nonlinear equations [38]:

$$\begin{aligned}(J_p + m_b l_b^2)\ddot{\vartheta} &= -m_b g l_b \cos\vartheta - D_p\dot{\vartheta} - m_b l_b^2 \dot{\varphi}^2 \sin\vartheta\cos\vartheta + K_{pp}V_p + K_{py}V_y \\ (J_y + m_b l_b^2\cos^2\vartheta)\ddot{\varphi} &= -D_y\dot{\varphi} + 2m_b l_b^2\dot{\vartheta}\dot{\varphi}\sin\vartheta\cos\vartheta + K_{yp}V_p + K_{yy}V_y\end{aligned} \tag{33}$$

where ϑ and φ denote pitch and yaw angles denoting the outputs of the system, respectively, $\dot{\vartheta}$ and $\dot{\varphi}$ denote angular velocities of pitch and yaw angles, respectively, J_p and J_y are the moments of inertia about the pitch and yaw, respectively, m_b is the total mass of the body, l_b is the distance between the center of mass and the origin of the body-fixed frame, g is the gravity acceleration, D_p and D_y are the viscous friction coefficients, K_{pp}, K_{py}, K_{yp}, and K_{yy} are the thrust torque constants, and V_p and V_y are the input voltages injected to the DC motors for controlling two propellers. The system parameters are given in Table 1.

Table 1. Parameters of the 2-DOF Helicopter system [38].

Symbol	Value	SI Unit
m_b	1.0750	kg· m^2
g	9.8065	m/s^2
l_b	0.002	m
J_p	0.0215	kg· m^2
J_y	0.0237	kg· m^2
D_p	0.0071	N/V
D_y	0.0220	N/V
K_{pp}	0.0220	N· m/V
K_{py}	0.0221	N· m/V
K_{yp}	−0.0227	N· m/V
K_{yy}	0.0022	N· m/V

By considering the quantized input saturation and defining the variables $x_{1,1} = \vartheta$, $x_{1,2} = \varphi$, $x_{2,1} = \dot{\vartheta}$, $x_{2,2} = \dot{\varphi}$, $v_1 = V_p$, and $v_2 = V_y$. Then, the system (33) can be rewritten in the MIMO nonlinear form (1):

$$\begin{aligned}\dot{\boldsymbol{x}}_1 &= \boldsymbol{x}_2 \\ \dot{\boldsymbol{x}}_2 &= \boldsymbol{f}(\bar{\boldsymbol{x}}_2) + \boldsymbol{g}(\bar{\boldsymbol{x}}_2)u(q(\boldsymbol{v})) \\ \boldsymbol{y} &= \boldsymbol{x}_1\end{aligned} \tag{34}$$

where $\boldsymbol{x}_1 = [x_{1,1}, x_{1,2}]^\top$, $\boldsymbol{x}_2 = [x_{2,1}, x_{2,2}]^\top$, $\boldsymbol{v} = [v_1, v_2]^\top$, and

$$\boldsymbol{f} = \begin{bmatrix} \frac{-m_b g l_b \cos x_{1,1} - D_p x_{2,1} - m l_b^2 x_{2,2}^2 \sin x_{1,1}\cos x_{1,1}}{J_p + m_b l_b^2} \\ \frac{-D_y x_{2,2} + 2m_b l_b^2 x_{2,1} x_{2,2} \sin x_{1,1}\cos x_{1,1}}{J_y + m_b l_b^2 \cos^2 x_{1,1}} \end{bmatrix}, \quad \boldsymbol{g} = \begin{bmatrix} \frac{K_{pp}}{J_p + m_b l_b^2} & \frac{K_{py}}{J_p + m_b l_b^2} \\ \frac{K_{yp}}{J_y + m_b l_b^2 \cos^2 x_{1,1}} & \frac{K_{yy}}{J_y + m_b l_b^2 \cos^2 x_{1,1}} \end{bmatrix}.$$

Notice that the unknown function matrix $\boldsymbol{g}$ in system (34) satisfies Assumption 1.

4.2. Design of Quantized-States-Based Adaptive Tracker

Define the augmented error using quantized states as

$$\boldsymbol{s}^* = \boldsymbol{z}_2^* + \boldsymbol{\Lambda}\boldsymbol{z}_1^* \tag{35}$$

where $\boldsymbol{s}^* = [s_1^*, s_2^*]^\top$, $\boldsymbol{z}_1^* = \boldsymbol{x}_1^* - \boldsymbol{x}_d$, $\boldsymbol{z}_2^* = \boldsymbol{x}_2^* - \dot{\boldsymbol{x}}_d - \boldsymbol{\Psi}\mathrm{Tanh}\boldsymbol{\phi}$, $\boldsymbol{x}_d = [x_{1,d}, x_{2,d}]^\top$, $\boldsymbol{\phi} = [\phi_1, \phi_2]^\top$, $\boldsymbol{\Psi} = \begin{bmatrix} \psi_1 & 0 \\ 0 & \psi_2 \end{bmatrix}$, and $\boldsymbol{\Lambda} = \begin{bmatrix} \lambda_1 & 0 \\ 0 & \lambda_2 \end{bmatrix}$. Here, $\boldsymbol{\phi}$ is given by

$$\dot{\phi}_j = (\cosh^2\phi_j)(-\kappa_j \tanh\phi_j + u(v_j^q) - v_j^q)/\psi_j, \quad \phi_j(0) = 0, \quad j = 1, 2. \tag{36}$$

Using the similar reasoning in Section 3.1, the adaptive quantized state feedback tracker for system (34) can be derived as follows:

$$\boldsymbol{v} = -\boldsymbol{\zeta}\boldsymbol{s}^* - \boldsymbol{\Lambda}\boldsymbol{z}_2^* + \boldsymbol{x}_d^{(n)} - \hat{\boldsymbol{W}}^\top \boldsymbol{Q}(\bar{\boldsymbol{x}}^q) - \hat{B}\text{Tanh}(\boldsymbol{s}^*/\epsilon) \tag{37}$$

$$\dot{\hat{\boldsymbol{W}}}_j = \boldsymbol{\Gamma}_{W,j}(s_j^* \boldsymbol{Q}_j(\bar{\boldsymbol{x}}^q) - \sigma_W |s_j^*| \hat{\boldsymbol{W}}_j), \quad j = 1,2 \tag{38}$$

$$\dot{\hat{B}} = \Gamma_B(\boldsymbol{s}^{*\top}\text{Tanh}(\boldsymbol{s}^*/\epsilon) - \sigma_B \|\boldsymbol{s}^*\| \hat{B}) \tag{39}$$

where $\boldsymbol{\zeta} = \begin{bmatrix} \zeta_1 & 0 \\ 0 & \zeta_2 \end{bmatrix}$ and $\boldsymbol{\Gamma}_{W,j} = \begin{bmatrix} \gamma_{w,1} & 0 \\ 0 & \gamma_{w,2} \end{bmatrix}$.

Remark 4. *In the existing nonlinear control results dealing with the 2-DOF helicopter system [38–41], the input saturation problem was not considered even though input saturation practically occurs in the 2-DOF helicopter system (34). Besides, the previous results [38–41] did not consider both the state and input quantization problems and thus cannot be applied to the network-based state-quantized control problem. However, this paper considers the state quantization and the quantized input saturation effects.*

4.3. Simulation Results

Prior to the implementation, a numerical simulation for system (34) is proceeded. The initial conditions for the simulations are set to $\boldsymbol{x}_1(0) = [-0.05, 0.05]^\top$ (rad/s) and $\boldsymbol{x}_2(0) = [0,0]^\top$. Hence, the input saturation of V_p and V_y are set to $u_{1,M} = u_{2,M} = 24$ from the DC motor specification. The length of the quantization intervals are chosen as $l = 0.01$ for state variables and $l = 1$ for control inputs. The design parameters are chosen as $\zeta_1 = \zeta_2 = 1, \lambda_1 = \lambda_2 = 3, \psi_1 = \psi_2 = 1, \kappa_1 = \kappa_2 = 200, \epsilon = 0.1, \gamma_{w,1} = \gamma_{w,2} = 10, \Gamma_B = 1$, and $\sigma_W = \sigma_B = 0.001$. The mean squared errors for the pitch and yaw angles are 0.1044 and 0.0435, respectively. The tracking results for simulation are shown in Figure 3. The DC motor voltages denoting the control inputs are shown in Figure 4. The output of RBFNNs and the estimation results of unknown parameter are displayed in Figure 5. From these figures, we show that the proposed adaptive quantized state feedback tracker achieves the robust tracking in the presence of state quantization and the quantized input saturation of the MIMO nonlinear system (34).

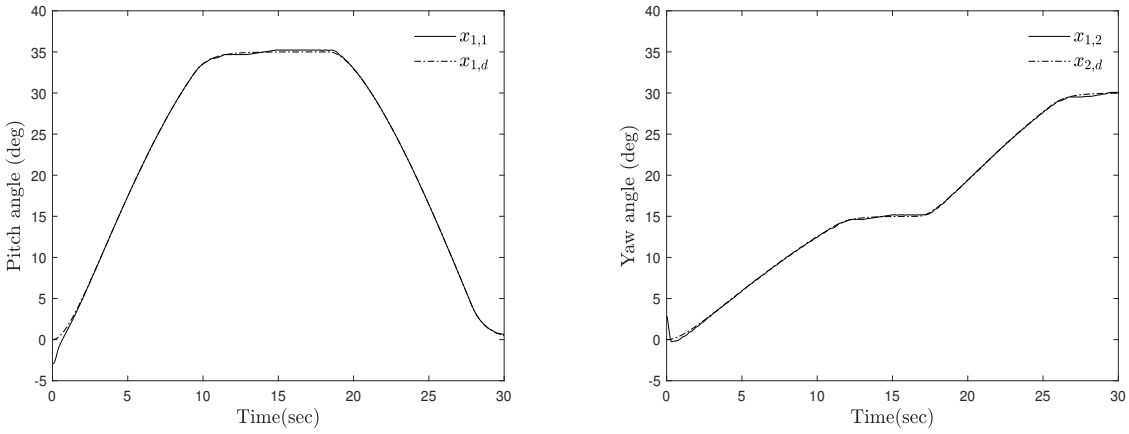

(**a**) (**b**)

Figure 3. Tracking results for simulation (**a**) $x_{1,1}$ and $x_{1,d}$ (**b**) $x_{1,2}$ and $x_{2,d}$.

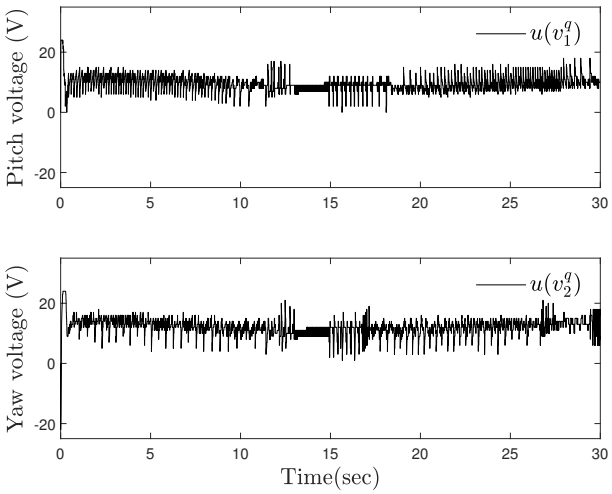

Figure 4. Control input voltages V_p and V_y for simulation.

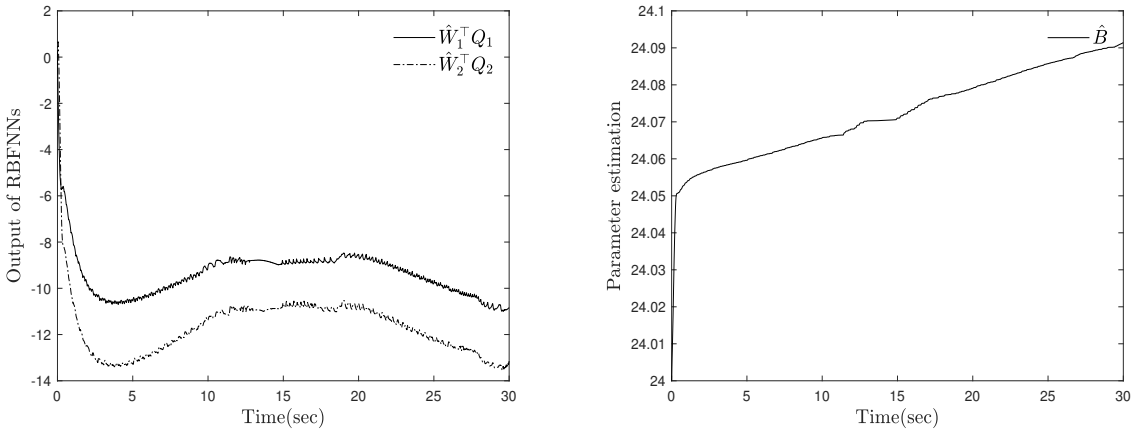

Figure 5. RBFNNs outputs and adaptive parameters for simulation (**a**) $\hat{W}_1^\top Q_1$ and $\hat{W}_2^\top Q_2$ (**b**) $\hat{B}$.

4.4. Experimental Results

The experiment setup is shown in Figure 6. The experiment results are displayed in Figures 7–9. The initial conditions for experiment are set to $x_1(0) = [0,0]^\top$(rad/s) and $x_2(0) = [0,0]^\top$. The input saturation is set as $u_{1,M} = u_{2,M} = 24$. The length of the quantization intervals are chosen as $l = 0.01$ for state variables and $l = 1$ for control inputs. The design parameters are chosen as $\zeta_1 = \zeta_2 = 30, \lambda_1 = \lambda_2 = 3, \psi_1 = \psi_2 = 1, \kappa_1 = \kappa_2 = 200, \epsilon = 1, \gamma_{w,1} = \gamma_{w,2} = 7, \Gamma_B = 1$, and $\sigma_W = \sigma_B = 10^{-5}$. The tracking results for the experiment are shown in Figure 7. The mean squared errors for the pitch and yaw angles are 0.0656 and 0.0523, respectively. Figure 8 shows the input voltages. The RBFNNs outputs and estimation results are displayed in Figure 9. From these figures, we can see that the proposed approach is successfully validated via the 2-DOF helicopter system (34).

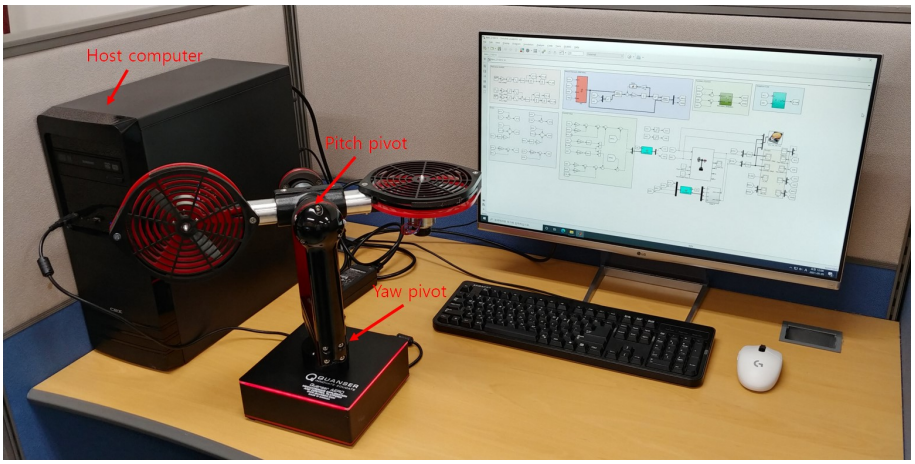

Figure 6. Experiment setup.

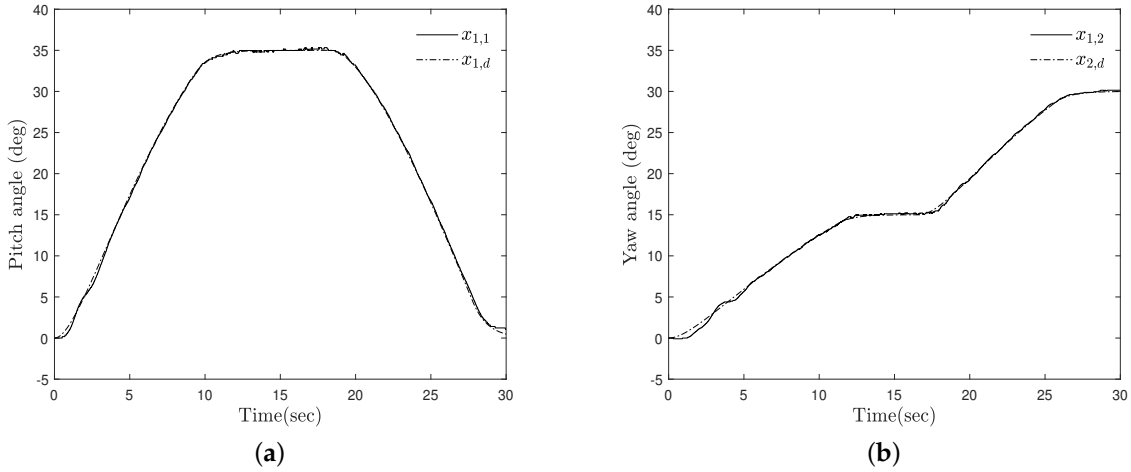

(a) **(b)**

Figure 7. Tracking results for experiment (**a**) $x_{1,1}$ and $x_{1,d}$ (**b**) $x_{1,2}$ and $x_{2,d}$.

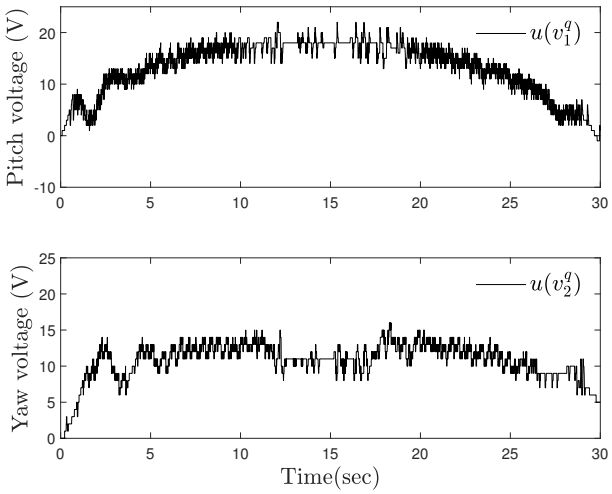

Figure 8. Control input voltage V_p and V_y for experiment.

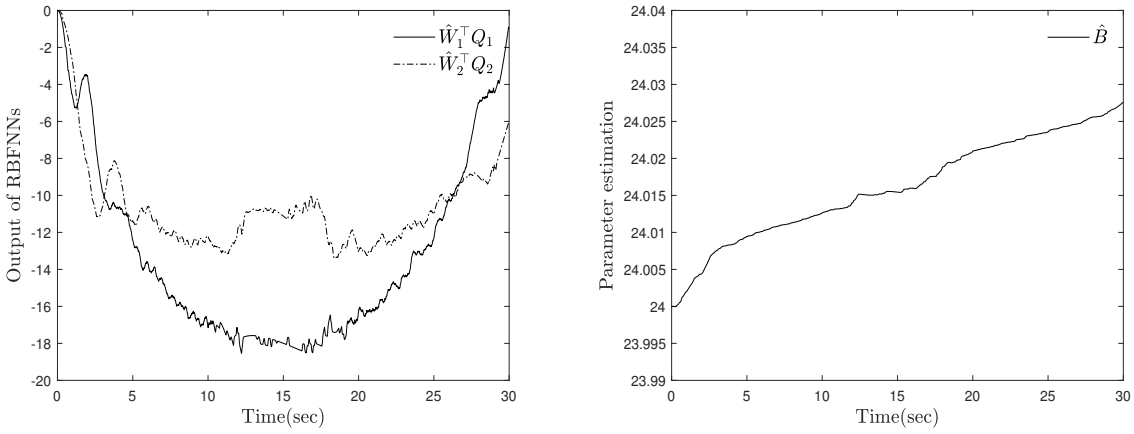

(**a**) (**b**)

Figure 9. RBFNNs outputs and adaptive parameters for experiment (**a**) $\hat{W}_1^\top Q_1$ and $\hat{W}_2^\top Q_2$ (**b**) $\hat{B}$.

5. Conclusions

A neural-network-based adaptive quantized state feedback control design has been developed for uncertain MIMO nonlinear systems with state quantization and quantized input saturation. In the design of the proposed tracker scheme, unknown system nonlinearities and quantization errors are compensated by RBFNNs and adaptive techniques, respectively. The auxiliary system using quantized states and compensation signals has been introduced to analyze the effects of the quantized multi-input saturation. The stability of the closed-loop error signals with quantization errors has been analyzed by some theoretical lemmas. Finally, we have validated the effectiveness of the proposed quantized state feedback tracker by presenting the simulation and experimental results for the 2-DOF helicopter system. Comparison studies of the adaptive neural tracker design to the deterministic artificial intelligence approach reported in [42] will be explored in the future.

Author Contributions: Conceptualization, methodology, software, writing—original draft preparation, B.M.K.; Conceptualization, methodology, writing—review and editing, supervision, S.J.Y. All authors have read and agreed to the published version of the manuscript.

Funding: This research was supported by the National Research Foundation of Korea (NRF) grant funded by the Korea government (NRF-2019R1A2C1004898).

Institutional Review Board Statement: Not applicable.

Informed Consent Statement: Not applicable.

Data Availability Statement: Not applicable.

Conflicts of Interest: The authors declare no conflict of interest.

References

1. Karason, S.P.; Annaswamy, A.M. Adaptive control in the presence of input constraints. *IEEE Trans. Autom. Cont.* **1994**, *39*, 2325–2330. [CrossRef]
2. Zhong, Y.S. Globally stable adaptive system design for minimum phase SISO plants with input saturation. *Automatica* **2005**, *41*, 1539–1547. [CrossRef]
3. Wen, C.; Zhou, J.; Liu, Z.; Su, H. Robust adaptive control of uncertain nonlinear systems in the presence of input saturation and external disturbance. *IEEE Trans. Autom. Cont.* **2011**, *56*, 1672–1678. [CrossRef]
4. Li, Y.; Tong, S.; Li, T. Composite adaptive fuzzy output feedback control design for uncertain nonlinear stric-feedback systems with input saturation. *IEEE Trans. Cyber.* **2015**, *45*, 2299–2308. [CrossRef] [PubMed]
5. Shi, S.; Tong, S.; Li, Y. Observer-based fuzzy adaptive prescribed performance trackingcontrol for nonlinear stochastic systems with input saturation. *Neurocomputing* **2015**, *158*, 100–108.
6. Gao, Y.F.; Sun, X.; Wen, C.; Wang, W. Adaptive tracking control for a class of stochastic uncertain nonlinear systems with input saturation. *IEEE Trans. Autom. Cont.* **2017**, *62*, 2498–2504. [CrossRef]

7. Gao, Y.F.; Sun, X.; Wen, C.; Wang, W. Oberver-based adaptive NN control for a class of uncertain nonlinear systems with nonsymmetric input saturation. *IEEE Trans. Nerual Netw. Learn. Syst.* **2017**, *28*, 1520–1530. [CrossRef]
8. Zhou, Q.; Wu, C.; Shi, P. Observer-based adaptive fuzzy tracking control of nonlinear systems with time delay and input saturation. *Fuzzy Sets Syst.* **2017**, *316*, 49–68. [CrossRef]
9. Zhang, Q.; Dong, J. Disturbance-observer-based adaptive fuzzy control for nonlinear state constrained systems with input saturation and input delay. *Fuzzy Sets Syst.* **2020**, *392*, 77–92. [CrossRef]
10. Wu, Y.; Xie, X. Robust adaptive control for state-constrained nonlinear systems with input saturation and unknown control direction. *IEEE Trans. Syst. Man Cyber. Syst.* **2021**, *51*, 1192–1202. [CrossRef]
11. Wang, Y.; Hu, J.; Wang, J.; Xing, X. Adaptive neural novel prescribed performance control for non-affine pure-feedback systems with input saturation. *Nonlinear Dyn.* **2018**, *93*, 1241–1259. [CrossRef]
12. Zerari, N.; Chemachema, M.; Essounbouli, N. Neural network based adaptive tracking control for a class of pure feedback nonlinear systems with input saturation. *IEEE/CAA J. Autom. Sin.* **2019**, *6*, 278–290. [CrossRef]
13. Chen, M.; Ge, S.S.; Ren, B. Adaptive tracking control of uncertain MIMO nonlinear systems with input constraints. *Automatica* **2011**, *47*, 452–465. [CrossRef]
14. Cui, G.; Yu, J.; Wang, Q. Finite-time adaptive fuzzy control for MIMO nonlinear systems with input saturation via inproved command-filtered backstepping. *IEEE Trans. Syst. Man Cyber. Syst.* **2020**. [CrossRef]
15. Si, W.; Dong, X. Adaptive neural control for MIMO stochastic nonlinear pure-feedback systems with input saturation and full-state constraints. *Neurocomputing* **2018**, *275*, 298–307. [CrossRef]
16. Sui, S.; Tong, S.; Li, Y. Adaptive fuzzy backstepping output feedback tracking control of MIMO stochastic pure-feedback nonlinear systems with input saturation. *Fuzzy Sets Syst.* **2014**, *254*, 26–46. [CrossRef]
17. Yang, Y.; Yue, D.; Yuan, D. Adaptive neural tracking control of a class of MIMO pure-feedback time-delay nonlinear systems with input saturation. *Int. J. Syst. Sci.* **2015**, *47*, 3730–3740. [CrossRef]
18. He, W.; Li, Z.; Dong, Y.; Zhao, T. Design and adaptive control for an upper limb robotic exoskeleton in presence of input saturation. *IEEE Trans. Nerual Netw. Learn. Syst.* **2019**, *30*, 97–108. [CrossRef]
19. Lian, F.L.; Moyne, J.R.; Tilbury, D.M. Performance evaluation of control networks: Ethernet, controlnet, and devicenet. *Control Syst. IEEE* **2001**, *21*, 66–83.
20. Zhou, J.; Wen, C.Y.; Yang, G.H. Adaptive backstepping stabilization of nonlinear uncertain systems with quantized input signal. *IEEE Trans. Autom. Control.* **2014**, *59*, 460–464. [CrossRef]
21. Lai, G.Y.; Liu, Z.; Philip Chen, C.L.; Zhang, Y. Adaptive asymptotic tracking control of uncertain nonlinear system with input quantization. *Syst. Control. Lett.* **2016**, *96*, 23–29. [CrossRef]
22. Li, Y.X.; Yang, G.H. Adaptive asymptotic tracking control of uncertain nonlinear systems with input quantization and actuator faults. *Automatica* **2016**, *72*, 177–185. [CrossRef]
23. Xing, L.T.; Wen, C.Y.; Su, H.Y. Robust control for a class of uncertain nonlinear systems with input quantization. *Int. J. Robust Nonlinear* **2016**, *26*, 1585–1596. [CrossRef]
24. Yu, X.W.; Lin, Y. Adaptive backstepping quantized control for a class of nonlinear systems. *IEEE Trans. Autom. Control.* **2017**, *62*, 981–985. [CrossRef]
25. Yang, Y.; Yu, Z.; Li, S. Adaptive output feedback quantised tracking control for stochastic nonstrict-feedback nonlinear systems with input saturation. *Int. J. Syst. Sci.* **2018**, *49*, 3130–3145. [CrossRef]
26. Xing, L.; Wen, C.; Liu, Z.; Cai, J.; Zhang, M. Adaptive control for a class of uncertain nonlinear systems subject to saturated input quantization. In Proceedings of the 2020 16th International Conference Control, Automation, Robotics and Vision (ICARCV), Shenzhen, China, 13–15 December 2020; pp. 472–477.
27. Zhou, J.; Wen, C.; Wang, W.; Yang, F. Adaptive backstepping control of nonlinear uncertain systems with quantized states. *IEEE Trans. Autom. Cont.* **2019**, *64*, 4756–4763. [CrossRef]
28. Choi, Y.H.; Yoo, S.J. Quantized feedback adaptive command filtered backstepping control for a class of uncertain nonlinear strict-feedback systems. *Nonlinear Dyn.* **2020**, *99*, 2907–2918. [CrossRef]
29. Choi, Y.H.; Yoo, S.J. Neural-networks-based adaptive quantized feedback tracking of uncertain nonlinear strict-feedback systems with unknown time delays. *J. Frankl. Inst.* **2020**, *357*, 10691–10715. [CrossRef]
30. Choi, Y.H.; Yoo, S.J. Quantized-feedback-based adaptive event-triggered control of a class of uncertain nonlinear systems. *Mathematic* **2020**, *8*, 1603. [CrossRef]
31. Meng, W.; Yang, Q.; Sun, Y. Adaptive neural control of nonlinear MIMO systems with time-varying output constraints. *IEEE Trans. Neural Netw. Learn. Syst.* **2015**, *26*, 1074–1085. [CrossRef]
32. Brockett, R.W.; Liberzon, D. Quantized feedback stabilization of linear systems. *IEEE Trans. Autom. Cont.* **2000**, *45*, 1279–1289. [CrossRef]
33. Polycarpou, M.M. Stable adaptive neural control scheme for nonlinear systems. *IEEE Trans. Autom. Cont.* **1996**, *41*, 447–451. [CrossRef]
34. Park, J.; Sandberg, I.W. Universal approximation using radial-basis-function networks. *Neural Comput.* **1991**, *3*, 246–257. [CrossRef]
35. Wang, C.; Hill, D.J.; Ge, G.G.; Chen, G. An ISS-modular approach for adaptive neural control of pure-feedback systems. *Automatica* **2006**, *42*, 625–635. [CrossRef]

36. Kurdila, A.J.; Narcowich, F.J.; Ward, J.D. Persistency of excitation in identification using radial basis function approximants. *SIAM J. Cont. Optim.* **1995**, *33*, 625–642. [CrossRef]
37. Quanser Inc. *Quanser AERO Laboratory Guide*; Technical Report; Quanser: Arkham, ON, Canada, 2016.
38. Labdai, S.; Chrifi-Alaoui, L.; Drid, S.; Delahoche, L.; Bussy, P. Real-time implementation of an optimized fractional sliding mode controller on the quanser-aero helicopter. In Proceedings of the 2020 International Conference Control, Automation and Diagnosis (ICCAD), Paris, France, 7–9 October 2020.
39. Lambert, P.; Reyhanoglu, M. Observer-based sliding mode control of a 2-DoF Helicopter system. In Proceedings of the IECON 2018 44th Annual Conference of the IEEE Industrial Electronics Society, Washington, DC, USA, 21–23 October 2018.
40. Schlanbusch, S.; Zhou, J. Adaptive backstepping control of a 2-DOF helicopter. In Proceedings of the 2019 IEEE 7th International Conference on Control, Mechatronics and Automation, Delft, The Netherlands, 6–8 November 2019.
41. Schlanbusch, S.; Zhou, J. Adaptive backstepping control of a 2-DOF helicopter system with uniform quantized inputs. In Proceedings of the IECON 2020 46th Annual Conference of the IEEE Industrial Electronics Society, Singapore, 18–21 October 2020.
42. Sands, T. Control of DC motors to guide unmanned underwater vehicles. *Appl. Sci.* **2021**, *11*, 2144. [CrossRef]